Journal of Theoretical Biology 261 (2009) 83–92

Contents lists available at ScienceDirect

Journal of Theoretical Biology

journal homepage: www.elsevier.com/locate/yjtbi

Spike latency and jitter of neuronal membrane patches with stochastic Hodgkin–Huxley channels

Mahmut Ozer [a,*], Muhammet Uzuntarla [a], Matjaž Perc [b], Lyle J. Graham [c,*]

[a] Zonguldak Karaelmas University, Engineering Faculty, Department of Electrical and Electronics Engineering, 67100 Zonguldak, Turkey
[b] University of Maribor, Faculty of Natural Sciences and Mathematics, Department of Physics, Koroška cesta 160, SI-2000 Maribor, Slovenia
[c] Laboratory of Neurophysics and Physiology, UMR 8119 CNRS, Université Paris Descartes, 45 rue des Saint-Peres, 75006 Paris, France

ARTICLE INFO

Article history:
Received 5 May 2009
Received in revised form
4 July 2009
Accepted 7 July 2009
Available online 15 July 2009

Keywords:
Ion channel noise
First spike
Stochastic resonance

ABSTRACT

Ion channel stochasticity can influence the voltage dynamics of neuronal membrane, with stronger effects for smaller patches of membrane because of the correspondingly smaller number of channels. We examine this question with respect to first spike statistics in response to a periodic input of membrane patches including stochastic Hodgkin–Huxley channels, comparing these responses to spontaneous firing. Without noise, firing threshold of the model depends on frequency—a sinusoidal stimulus is subthreshold for low and high frequencies and suprathreshold for intermediate frequencies. When channel noise is added, a stimulus in the lower range of subthreshold frequencies can influence spike output, while high subthreshold frequencies remain subthreshold. Both input frequency and channel noise strength influence spike timing. Specifically, spike latency and jitter have distinct minima as a function of input frequency, showing a resonance like behavior. With either no input, or low frequency subthreshold input, or input in the low or high suprathreshold frequency range, channel noise reduces latency and jitter, with the strongest impact for the lowest input frequencies. In contrast, for an intermediate range of suprathreshold frequencies, where an optimal input gives a minimum latency, the noise effect reverses, and spike latency and jitter increase with channel noise. Thus, a resonant minimum of the spike response as a function of frequency becomes more pronounced with less noise. Spike latency and jitter also depend on the initial phase of the input, resulting in minimal latencies at an optimal phase, and depend on the membrane time constant, with a longer time constant broadening frequency tuning for minimal latency and jitter. Taken together, these results suggest how stochasticity of ion channels may influence spike timing and thus coding for neurons with functionally localized concentrations of channels, such as in "hot spots" of dendrites, spines or axons.

1. Introduction

Neurons transmit information about their inputs by transforming them into the spike trains, and it is likely that the processing capacity of neurons is directly connected to the detailed nature of these trains as a code (Schneidman et al., 2000). In principle, information in spike trains may be encoded in either the timing of the spikes (Kruger and Becker, 1991; Tovée et al., 1993; Middlebrooks et al., 1994) or in the average firing rate (de Ruyter van Steveninck and Bialek, 1988). However, codes based on spike timing can make more efficient use of the capacity of neural connections than those that rely simply on the firing rate (Vanrullen et al., 2005; Butts et al., 2007). In this context, studying first spike latency following stimulus onset is an important subject for the physiology of neural function, and has been examined with experimental protocols using current injection (Chen et al., 1996) or sensory stimulation (Philips, 1998; Heil, 2004), as well as with theoretical studies investigating the roles of different biophysical mechanisms. Panzeri et al. (2001) investigated how spike timing can code stimulus position, and found that under certain conditions complex, single neuron spike patterns provide much less information about where a stimulus has occurred than the first spike time. In a theoretical study, Tuckwell and Wan (2005) described an analytical approach for determining the time to first spike from a given initial state with a standard 4-component Hodgkin–Huxley (H–H) model and its 2-component approximation model. Tuckwell (2005) then studied the time to first spike for both models driven by a Gaussian noise with non-zero drift and variance parameters, and found that the sample paths in the 2-component approximation model were very close to those of the 4-component model if the time to spike

* Corresponding authors. Tel.: +90 372 257 5446, fax: +90 372 257 4023 (Mahmut Ozer); tel.: +33 1 42 86 20 92, fax: +33 1 49 27 90 62 (Lyle J. Graham).
E-mail addresses: mahmutozer2002@yahoo.com (M. Ozer), lyle@biomedicale.univ-paris5.fr (L.J. Graham).

0022-5193/$ - see front matter © 2009 Elsevier Ltd. All rights reserved.
doi:10.1016/j.jtbi.2009.07.006

is small. Pankratova et al. (2005a) recently analyzed the influence of external noise on the latency of the first spike based on the stochastic FitzHugh–Nagumo model subject to a strong periodic input, and showed that noise increases the first spike latency and thus delays signal detection, an effect called "noise delayed decay" (NDD). This study also showed that a proper choice of the forcing parameters (thus, the input) could minimize the delay due to noise. Pankratova et al. (2005b) reconsidered the subject for an H–H neuronal model driven by a noisy suprathreshold periodic forcing and obtained similar results. In a recent study, we investigated the noise-induced increase in the latency of the first spike, and showed that the NDD effect on spike latency near the frequency boundaries of a suprathreshold spiking regime depends not only on noise, but is also a function of the overall activity of the network (Ozer and Graham, 2008).

These models (Pankratova et al., 2005a, 2005b; Ozer and Graham, 2008) considered noise from an external additive current source. From a biophysical standpoint, however, an important consideration is that the dynamics of the voltage gated ion channels underling spike generation in excitable membranes are stochastic. Thus, fluctuations of the number of open ion channels around the corresponding mean values give rise to random conductance fluctuations. Theoretical analysis by Lecar and Nossal (1971) showed that these microscopic fluctuations could cause macroscopic threshold fluctuations in neurons, a prediction later verified experimentally by Sigworth (1980). Work by various groups has shown how channel stochasticity can modify excitability, cause spontaneous firing and result in variability in spike timing as well as interspike intervals (Skaugen and Walloe, 1979; Strassberg and DeFelice, 1993; Rubinstein, 1995; Chow and White, 1996; Schneidman et al., 1998; White et al., 2000). Channel noise can also provide improvements in the representation of weak signals through stochastic resonance (SR) (Bezrukov and Vodyanov, 1995; Levin and Miller, 1996). In a recent study, we examined the effect of the channel noise on the time-course of recovery from inactivation of sodium channels, and showed that it provides a non-zero proportion of non-inactivated channels as well as a faster time for recovery from inactivation (Ozer and Ekmekci, 2005) when compared to the deterministic model.

The effects of the channel noise depends on the membrane patch size for a given channel density. When the patch size is large enough, stochastic effects of the channel noise becomes negligible and the collective dynamics approaches the deterministic description. However, when the patch size is small—specifically, when the number of channels is small-stochastic effects of the individual channels have a significant effect on the membrane dynamics. Recently, it has been suggested that weak signals may be better detected by clusters of the ion channels in patches around $1\,\mu m^2$ through SR (Jung and Shuai, 2001; Schmid et al., 2001). Therefore, by tuning the patch size, resonance effects are obtained that may be relevant for neuronal information encoding (Schmid et al., 2004). The effect of patch temperature on spontaneous firing have also been examined for small membrane patches, and a remarkable temperature-dependent coherence resonance region has been found for patches between 0.3 and $5\,\mu m^2$ (Yang and Jia, 2005). Recently, Ozer (2006) investigated the effect of the sub-threshold periodic current forcing on the regularity and synchronization of neuronal spiking activity with a model that included channel noise, and showed that the regularity of spike trains exhibits two resonances which are independent of the forcing frequency for very small patch sizes but dependent on the frequency for larger membrane patch sizes.

Thus, among other effects, channel noise arising in small membrane patches will affect both the latency of the first spike and its variability. In this study we further examine this question with a stochastic ion channel model, studying how latency in response to subthreshold and suprathreshold periodic forcing depends on noise strength, the frequency and initial phase of the input, and the membrane time constant.

2. Model and methods

In Hodgkin and Huxley (1952) model, the time evolution of membrane potential is given by

$$C_m\,dV/dt + G_{Na}(V-E_{Na}) + G_K(V-E_K) + G_L(V-E_L) = I_{ext} \quad (1)$$

where V is the membrane potential, $C_m = 1\,\mu F\,cm^{-2}$ is the membrane capacity and I_{ext} is an externally applied current; $I_{ext}(t) = A\sin(\omega t+\varphi)$, where A, φ and ω denote the amplitude, phase and angular frequency of the sinusoidal forcing current, respectively. G_{Na}, G_K and G_L represent sodium, potassium and leakage conductances, respectively. $E_{Na} = 50\,mV$, $E_K = -77\,mV$ and $E_L = -54.4\,mV$ are the reversal potentials for the sodium, potassium and leakage channels, respectively. In the model, the leakage conductance is assumed to be constant, $G_L = 0.3\,mS\,cm^{-2}$, while the sodium and potassium conductances dynamically change according to the following equation:

$$G_{Na} = g_{Na}^{max} m^3 h, G_K = g_K^{max} n^4 \quad (2)$$

where $g_{Na}^{max} = 120\,mS\,cm^{-2}$ and $g_K^{max} = 36\,mS\,cm^{-2}$ are the maximal sodium and potassium conductances, respectively. m and h denotes activation and inactivation gating variables for the sodium channel, respectively. The potassium channel includes an activation gating variable n. Consequently, m^3h indicates the mean proportion of the open sodium channels in a membrane patch, and n^4 is the mean proportion of the open potassium channels.

The effects of channel noise have been modeled by using different computational algorithms including those proposed by Strassberg and DeFelice (1993), Rubinstein (1995), Chow and White (1996), and Fox (1997). While it has been shown that these different methods provide similar results (Mino et al., 2002), the actual correspondence to reality of any of the algorithms remains unknown (Rowat and Elson, 2004). In our study we used the algorithm presented by Fox (1997) both because it is widely used (Schmid et al., 2001, 2003, 2004, 2007; Rowat and Elson, 2004; Ozer et al., 2006, 2008, 2009) and because it is more computationally efficient than the other algorithms. Since we considered a large range of the model parameters (patch size, input frequency, input phase), this latter consideration is important. The approach put forward by Fox (1997) expresses the gating variable dynamics with the corresponding Langevin generalization, which contribute to the voltage-dependent first-order differential equations for the activation and inactivation gating variables, m, n and h originally proposed by Hodgkin and Huxley (1952):

$$dx/dt = \alpha_x(1-x) - \beta_x x + \xi_x(t), x = m,n,h \quad (3)$$

where α_x and β_x are rate functions for the gating variable x. The probabilistic nature of the channels appears as a noise source in Eq. (3), $\xi_x(t)$, which is an independent zero mean Gaussian white noise source whose autocorrelation function is given as follows (Fox, 1997):

$$\langle \xi_m(t)\xi_m(t')\rangle = \{2\alpha_m\beta_m/[N_{Na}(\alpha_m+\beta_m)]\}\delta(t-t') \quad (4)$$

$$\langle \xi_h(t)\xi_h(t')\rangle = \{2\alpha_h\beta_h/[N_{Na}(\alpha_h+\beta_h)]\}\delta(t-t') \quad (5)$$

$$\langle \xi_n(t)\xi_n(t')\rangle = \{2\alpha_n\beta_n/[N_K(\alpha_n+\beta_n)]\}\delta(t-t') \quad (6)$$

where N_{Na} and N_K represent total number of the sodium and potassium channels within a membrane patch, respectively. Given the assumption of homogeneous sodium and potassium ion

channel densities, channel numbers are calculated by $N_{Na} = \rho_{Na}S, N_K = \rho_K S$, where $\rho_{Na} = 60\,\mu m^{-2}$ and $\rho_K = 18\,\mu m^{-2}$ are the sodium and potassium channel densities, respectively, and S represents total membrane area (Fox, 1997; Schmid et al., 2003; Ozer, 2006; Ozer et al., 2006). Eqs. (1)–(6) constitute the stochastic H–H model, where the membrane area S globally determines the intrinsic noise level. In the simulation results presented below, the amplitude of the forcing input is fixed at $10\,\mu A\,cm^{-2}$.

We define the latency to the first spike as the time of the first upward crossing of the membrane potential past a fixed detection threshold value, taken here equal to 10 mV, relative to the start of the simulation, whether there was a forcing input or not (spontaneous firing case). We obtain the mean latency (ML) of an ensemble of first spikes by averaging their latencies over N realizations as follows:

$$ML = \langle t \rangle = N^{-1} \sum_{i=1}^{N} t_i \tag{7}$$

where t_i is the response time for i-th realization. We also consider the standard deviation of the latencies as follows:

$$\sigma_L = \sqrt{\langle t^2 \rangle - \langle t \rangle^2} \tag{8}$$

where $\langle t^2 \rangle$ represents the mean squared latency. In order to calculate ML, we averaged the first spike latencies over $N = 1000$ realizations. The numerical integration of the stochastic H–H model is performed using the standard stochastic Euler algorithm with a step size of 2 μs (Schmid et al., 2003; Ozer, 2006; Ozer et al., 2006).

3. Results

3.1. Dependence of latency and jitter on channel noise during spontaneous firing

We first examined the behavior of the model in the absence of input. The neuronal membrane fires spontaneously due to the intrinsic channel noise with a firing rate that increases with an increase in the noise level, i.e. with a decrease in the size of the patch (Fig. 1), ranging from 1.72 ± 0.17 Hz for a $64\,\mu m^2$ patch, to 68.9 ± 0.77 Hz for a $0.5\,\mu m^2$ patch (frequencies averaged over 50 trials of 50 s duration). The minimum sodium current for generating an action potential is proportional to the admittance of the membrane, which in the model scales as the membrane area since all membrane properties are expressed as densities. Therefore, since the sodium conductance scales with area, this means that for a (minimum) fixed sodium channel density there is sufficient sodium current for spike generation, independent of patch size. The mean latency to the first spike, measured from the start of a stimulation trial, showed a similar dependence on noise, thus decreasing with smaller patch sizes, ranging from 7.2 ± 7 ms ($0.5\,\mu m^2$ patch) to 16300 ± 15400 ms ($128\,\mu m^2$ patch). Although this latency measure varies considerably with patch size, the relative precision is fairly constant (CV∼1).

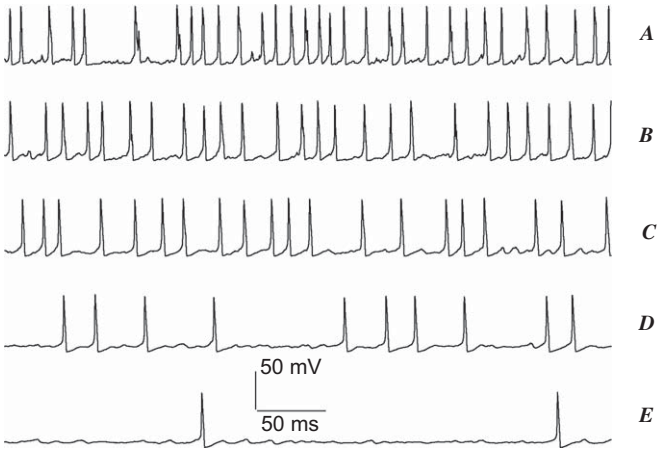

Fig. 1. Sample voltage traces for five different patch sizes in the absence of external stimuli: (a) 0.5, (b) 1, (c) 4, (d) 16, and (e) $32\,\mu m^2$.

The spike latency statistics for the spontaneous firing case provide a benchmark for the model when driven by a sinusoidal stimulus, as described below. Thus, we can consider the stimulus ineffective at driving the membrane at some given frequency if the mean spike latency (and jitter) is equivalent to the spontaneous firing case.

3.2. Dependence of latency and jitter on channel noise and input frequency

We then investigated spike latency and jitter of the model in response to a periodic current input, over a broad range of frequencies from 0.15 Hz to 3 kHz, and with different levels of channel noise. In the deterministic limit of large S values, the firing current threshold of the H–H model changes in a frequency-dependent manner (Schmid et al., 2003), notably being larger at both lower as well as higher frequencies. Below a critical amplitude, which in the model studied here is around $1.5\,\mu A\,cm^{-2}$, however, the model does not fire for any input frequency. Above this amplitude, the phase diagram of firing exhibits transitions between spiking and non-spiking regimes reflecting a typical hysteresis character (see Schmid et al., 2003, Fig. 12.1). As the frequency of the periodic forcing increases, the model passes first through a subthreshold non-spiking regime (first region of the frequency range), then a suprathreshold spiking regime (second region of the frequency range), and finally another subthreshold non-spiking regime (third region of the frequency range). For the model studied here, using a sinusoidal current forcing of magnitude of $10\,\mu A\,cm^{-2}$, the three subthreshold, suprathrehold and subthreshold regimes span 0.15–5 Hz, 5–350 Hz, and 350 Hz–3 kHz, respectively (Fig. 2).

We calculated the mean latencies (Fig. 2a) and their standard deviations σ_L, henceforth called jitter (Fig. 2b), for patch sizes ranging from 0.5 to $64\,\mu m^2$ over all frequencies with the initial phase of the input set to zero ($\varphi = 0$), as well as for a larger range of patch sizes spanning 0.5–$256\,\mu m^2$ for mid frequency suprathreshold inputs (Fig. 3). The qualitative distinction between effective and ineffective input in the presence of noise as a function of frequency is illustrated in Figs. 2c and d, where the latency and jitter in response to sinusoidal input for different patch sizes is plotted relative to the values for the undriven case—when these relative measures approach one, then the stimulus can be considered as ineffective.

Mean spike latency exhibits both similar and different characteristics when comparing the lower and upper subthreshold frequency ranges. The maximal mean latencies in these two subthreshold regions ranged from 6.6 and 6.8 ms, respectively ($0.5\,\mu m^2$ patch), to 185 and 618 ms, respectively ($64\,\mu m^2$ patch), thus for both frequency ranges intrinsic noise decreases the mean latency of spiking, similarly to that observed in the absence of current stimulation in Fig. 1. For low frequency subthreshold inputs, mean latency depends on both the input frequency and the channel noise, with the frequency dependence dominating over the channel noise as the frequency increases. In comparison, for high frequency subthreshold inputs, spike latency is more

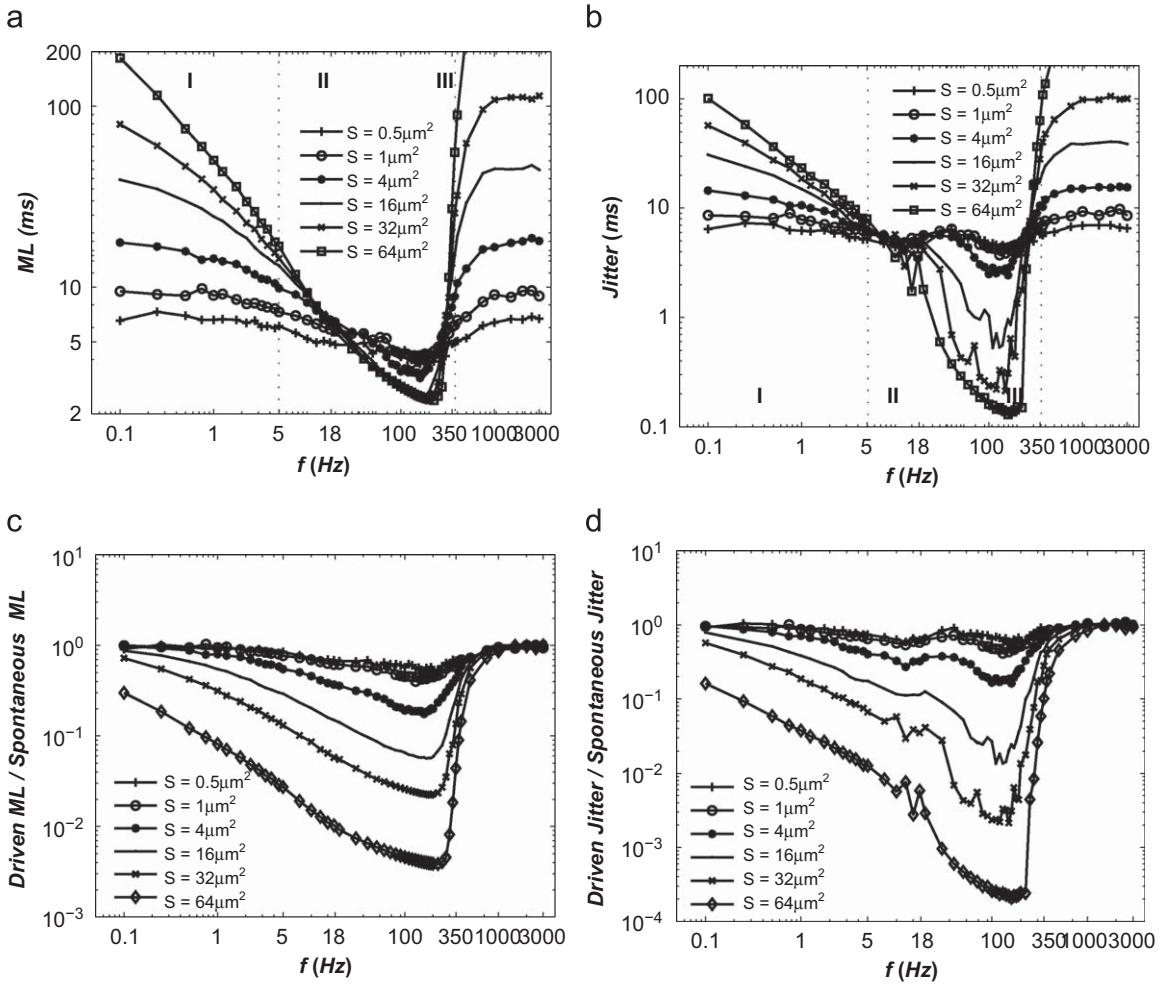

Fig. 2. The statistics of latency for six different patch sizes (0.5, 1, 4, 16, 32 and 64 μm^2) and 50 different frequencies of the forcing in the range of 0.15 Hz–3 kHz: (a) the mean latency versus the frequency, (b) the temporal jitter versus the frequency: in both panels I is the first subthreshold regime at low frequencies spanning 0.15–5 Hz, II is the suprathreshold regime between 5 and 350 Hz, and III is the second subthreshold regime at high frequencies of 350–3 kHz, (c) mean latency normalized to spontaneous firing case, and (d) mean jitter normalized to spontaneous firing case.

dependent on the channel noise, and is always greater than or equal to the corresponding values at lower frequencies. In this range, as the frequency increases, spike latency approaches the value obtained without input, implying that the stimulus has no effect on firing.

The shorter latencies for lower input frequencies is in qualitative agreement with computational results indicating that noisy spike encoders encode slowly varying stimuli more effectively than rapid ones, when compared using a statistical measure called the coding fraction (Steinmetz et al., 2001). Measurements of the coding fraction for sinusoidally varying inputs in cortical pyramidal cells also support that result (Fellous et al., 2001). Although the neuron tends to fire the first spike within the first cycle of the input in the slow frequency subthreshold region, the first spike typically occurs after several cycles (cycle skipping) for high frequency subthreshold inputs, again consistent with the interpretation that high frequency stimuli has little effect on spike timing. A recent study also showed that the cycle skipping leads to first-spike latency increases and apparent jitter even without noise in the θ-neuron model (Brumberg and Gutkin, 2007).

For mid-frequency suprathreshold inputs, the mean latency exhibits a resonance-like behavior with a minimum value for optimal frequencies ranging from 125 to 200 Hz. This resonance behavior of spike latency in the suprathreshold regime is similar to the results of Pankratova et al. (2005b), although that study reported a lower resonance frequency range of 90–120 Hz. The optimal frequency decreases as the noise increases [see Fig. 3(a)]. Interestingly, the corresponding minimum mean latencies also decrease with decreasing channel noise, with values ranging from 4 (0.5 μm^2 patch) to 2.4 ms (256 μm^2 patch), which is opposite to the general effect of more noise giving shorter latencies for the remainder of the input frequency spectrum.

The dependence of first spike jitter on noise and frequency follow that of the mean latency, as shown in Figs. 2 and 3. These figures show that in the first and third subthreshold regions, spike time jitter for a given patch size is roughly equal to the mean latency (compare with Fig. 2), which suggests that the neuronal membrane fires with lower absolute temporal precision for larger latencies. As with the mean latency, spike jitter in the second suprathreshold region also exhibits a resonance-like behavior at similar frequencies around 125–200 Hz, with minimum jitters ranging from 4.34 (0.5 μm^2 patch) to 0.07 ms (256 μm^2 patch). As the case with spike latency, a larger channel noise increases jitter in the vicinity of the resonance minima, while having the opposite effect for frequencies far from resonance [see Fig. 3(b)]. As with spike latency, the resonant behavior of the spike jitter also recapitulates the results of Pankratova et al. (2005b), although once again the resonance frequencies in that study were lower, spanning 60–90 Hz.

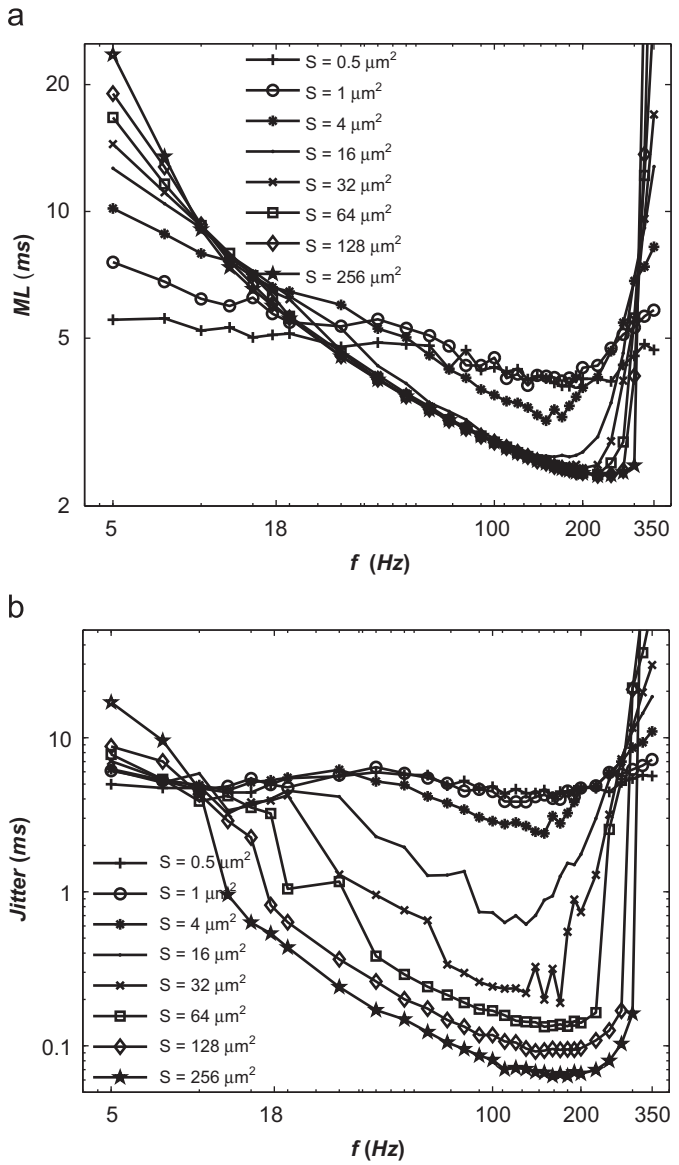

Fig. 3. The statistics of the latency for eight different patch sizes (0.5, 1, 4, 16, 32, 64, 128 and 256 μm^2) versus the forcing frequency in the suprathreshold regime: (a) the mean latency versus the frequency and (b) the temporal jitter versus the frequency.

Thus, channel noise has a detrimental effect on the response in the sense of increasing first spike latency and jitter for input frequencies between ~18 and 300 Hz. Since jitter increases with noise for these frequencies, the width of this band for any fixed value of the jitter increases with less noise, e.g. the frequency band for which first spike jitter is below 1 ms expands from 90–160 Hz for a patch size of 16 μm^2 to 13–300 Hz for a patch size of 256 μm^2. At the same time, compared to the entire range of input frequencies, first spike timing is fastest and more precise within this frequency range at any given noise level. Jitter decreases steeply as a function of frequency for inputs between 18 and 100 Hz, but much less so for higher frequencies up to about 200 Hz. This behavior is related to a change in phase-locking regimes, being 1:1 for a range of 18–100 Hz and n:1 for a range of 100–350 Hz (i.e. the membrane responded with a single spike over several stimulus cycles). Above about 200 Hz, jitter increases steeply with increasing frequency. These results indicate that the largest decrease in latency and jitter with increasing frequency occurs within the 1:1 phase locking regime, although the optimal input frequencies (125–200 Hz) are outside this mode, as reported by Pankratova et al. (2005b) using an input magnitude of 4 $\mu A\,cm^{-2}$.

The fact that the range of resonance frequencies for mean latency is the same as that for jitter gives a wide bandwidth for optimal first spike responses. In comparison, the resonant frequencies for latency and jitter in the model of Pankratova et al. (2005b)—identical to the one explored here apart from the source of noise-overlap only in a narrow range of frequencies around 90 Hz, resulting in a much more narrow optimal frequency band. We investigated if this difference may stem from the amplitude difference of the applied suprathreshold periodic forcing, since the periodic forcing in Pankratova et al. (2005b) had a magnitude of 4 $\mu A\,cm^{-2}$, compared to 10 $\mu A\,cm^{-2}$ used in the present study. However, when we repeated the simulations with a magnitude of 4 $\mu A\,cm^{-2}$ (results not shown), we again obtained a frequency range of optimal input frequencies for latency and jitter (~75–100 Hz) that was broader than that of Pankratova et al. (2005b).

The finding that the optimal frequency band enlarges and shifts towards higher values as the input increases (e.g. from 4 to 10 $\mu A\,cm^{-2}$) recapitulates the electrophysiological study by Fellous et al. (2001). That work examined the spike-time reliability of cortical neurons in response to sinusoidal currents of varying frequency and amplitude, finding that the frequency eliciting the highest reliability increased with increasing current amplitude. Similar results were also reported by theoretical studies using integrate-and-fire neurons (Hunter et al., 1998) and stochastic θ-neuron (Gutkin et al., 2003).

3.3. Dependence of latency and jitter on the initial input phase

We then examined the effect of the initial phase of the periodic forcing on spike latency and jitter in the subthreshold and suprathreshold inputs, thus frequencies of $f = 2.0$ Hz (Fig. 4), 160 Hz (Fig. 5) and 400 Hz (Fig. 6), corresponding to the first, second and third input frequency regions, respectively. Note that the suprathreshold frequency of 160 Hz falls within the resonance band described in the previous section that gives minimal values of latency and jitter.

For all three input frequencies, mean spike latency first decreases, then increases and then decreases again as a function of initial phase, thus giving a minimal latency at an optimal initial phase. This dependency is pronounced for the inputs falling within the low frequency subthreshold (Fig. 4) and the mid-frequency suprathreshold (Fig. 5) regimes, but negligible for the input in the high frequency subthreshold region (Fig. 6), once again consistent with the observation that inputs in this latter range are essentially ineffective at driving the membrane, even with noise.

For the input within the first subthreshold region (Fig. 4), the minimum mean latency as a function of initial phase was only weakly dependent on noise, ranging from 1.83 (128 μm^2 patch) to 2.5 ms (1 μm^2 patch), with an optimal initial phase of $\phi \sim \pi/2$ for all patch sizes. In contrast, at non-optimal initial phases, spike latency could be strongly influenced by noise. For example, with an initial phase of zero, the mean latency at 2.0 Hz ranged from 43.3 (128 μm^2 patch) to 8 ms (1 μm^2 patch). On the other hand, the behavior of jitter as a function of noise and initial phase was essentially opposite to that of the latency. Thus, jitter was most sensitive to noise at an initial phase that gave the minimum jitter ($\phi \sim \pi/2$ at all noise values), ranging from 0.06 (128 μm^2 patch) to 2.5 ms (1 μm^2 patch). In comparison, for an non-optimal initial phase of $\phi = 0$ the jitter was much less sensitive to noise, ranging from 17.5 (128 μm^2 patch) to 6.9 ms (1 μm^2 patch). Overall, for the

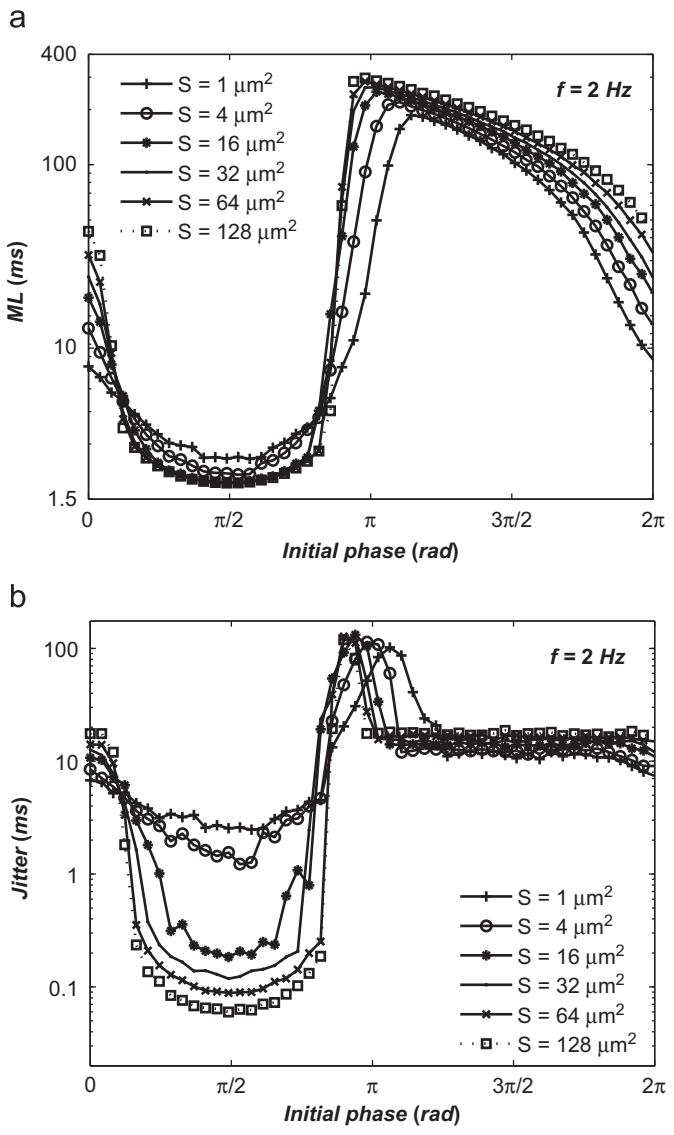

Fig. 4. The change of the latency in dependence on the initial phase of the periodic forcing within the first subthreshold regime, $f = 2$ Hz: (a) the mean latency versus the initial phase and (b) the temporal jitter versus the initial phase.

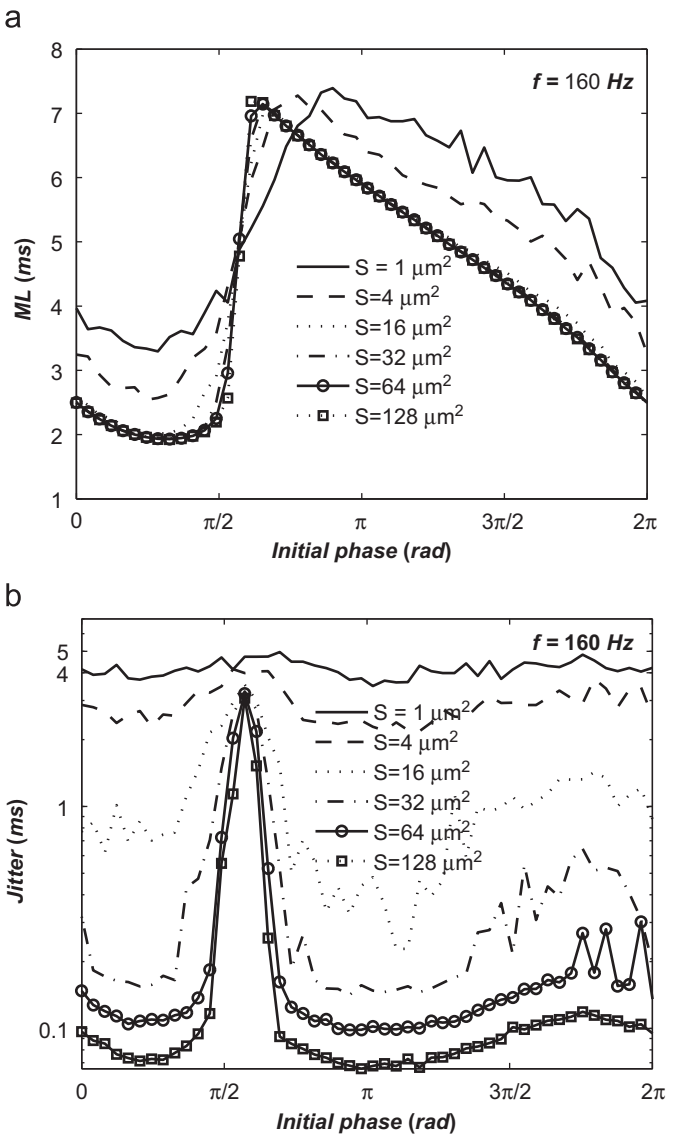

Fig. 5. The change of the latency in dependence on the initial phase of the periodic forcing within the suprathreshold regime, $f = 160$ Hz: (a) the mean latency versus the initial phase and (b) the temporal jitter versus the initial phase.

larger patch sizes, i.e. for smaller channel noise, an optimal initial phase of $\phi \sim \pi/2$ resulted in a 13 to 24-fold decrease in the mean latency and 100 to 300-fold decrease in the jitter, as compared to the case of $\phi = 0$, with a smaller relative difference for larger channel noise.

Earlier, we showed that when the initial phase is zero, spike latency and jitter decrease with an increase in channel noise in the low frequency subthreshold region. In contrast, for a range of initial phases that straddle the optimal phase ($\phi = 0.16\pi$–0.82π), this dependence reverses such that noise increases latency and jitter, similar to the switch in noise dependence over a band of frequencies in the suprathreshold input region. For initial phases larger than 0.82π there is a substantial increase both latency and jitter, which follows from the periodic forcing having smaller values near $\phi = \pi$ thus allowing the channel noise to dominate the response timing. As the initial phase increases, while the mean latency decreases the jitter takes an almost constant value near to that obtained for an initial phase of $\phi = 0$ (ranging from 7.5 ms for a 1 μm^2 patch, to 17 ms for a 128 μm^2 patch). To our knowledge, this is the first presentation of these diverse characteristics on the mean latency and jitter as a function of input phase in the low frequency subthreshold region.

In the suprathreshold region with $f = 160$ Hz, the minimal values of the mean latency as the initial phase was varied ranging from 1.92 (128 μm^2 patch) to 3.3 ms (1 μm^2 patch) (Fig. 5). The minima for the suprathreshold input occurred for a small range of values of the initial phase, between $\pi/5$ and $\pi/3$, in contrast to the essentially fixed optimal phase for the case of the low frequency subthreshold input, with larger optimal phases for lower values of the channel noise. Also in contrast to the subthreshold case, these mean latencies were not much lower than those obtained for an initial phase of zero, which ranged from 2.49 (128 μm^2 patch) to 3.97 ms (1 μm^2 patch). Thus, for an input of 160 Hz the optimal initial phases gave approximately a 1.3-fold decrease in the mean latency as compared to $\phi = 0$ for the larger patch sizes, i.e. for smaller channel noise. At an initial phase of around $\phi = 0.57\pi$ the dependence of channel noise on latency disappears, and for a small range of phases above this value larger channel noise tends to reduce latency. The maximal values of the mean latency occur for initial phases between $\phi = \pi/2$–π, with the maxima occurring at larger initial phases with increasing channel noise.

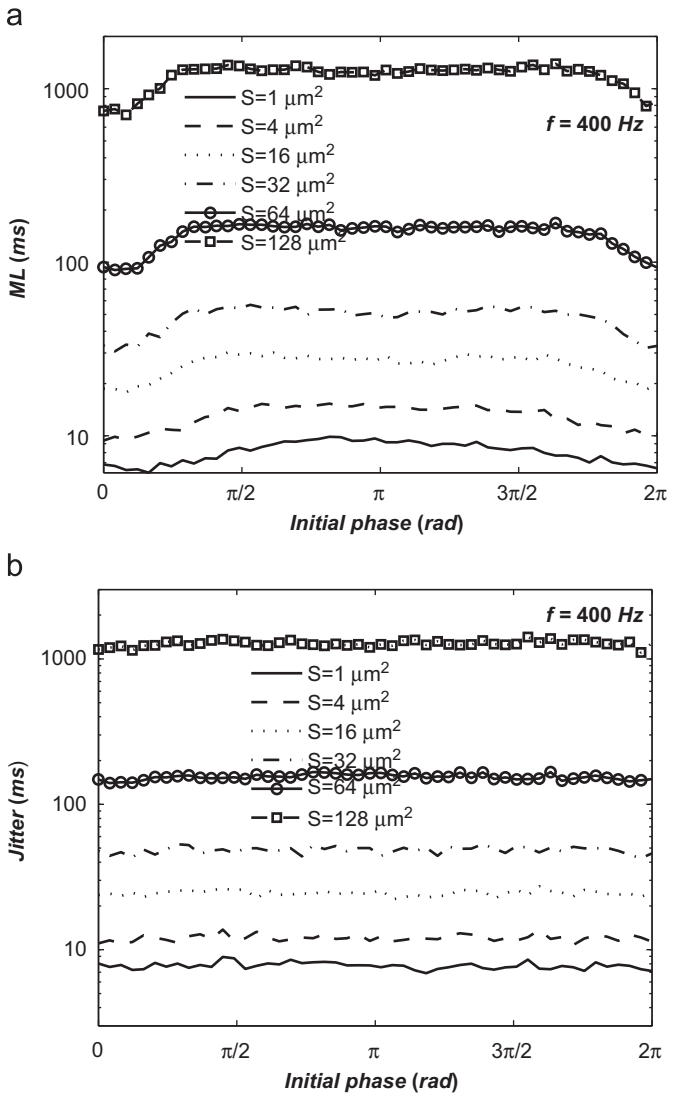

Fig. 6. The change of the latency in dependence on the initial phase of the periodic forcing within second subthreshold regime, $f = 400$ Hz: (a) the mean latency versus the initial phase and (b) the temporal jitter versus the initial phase.

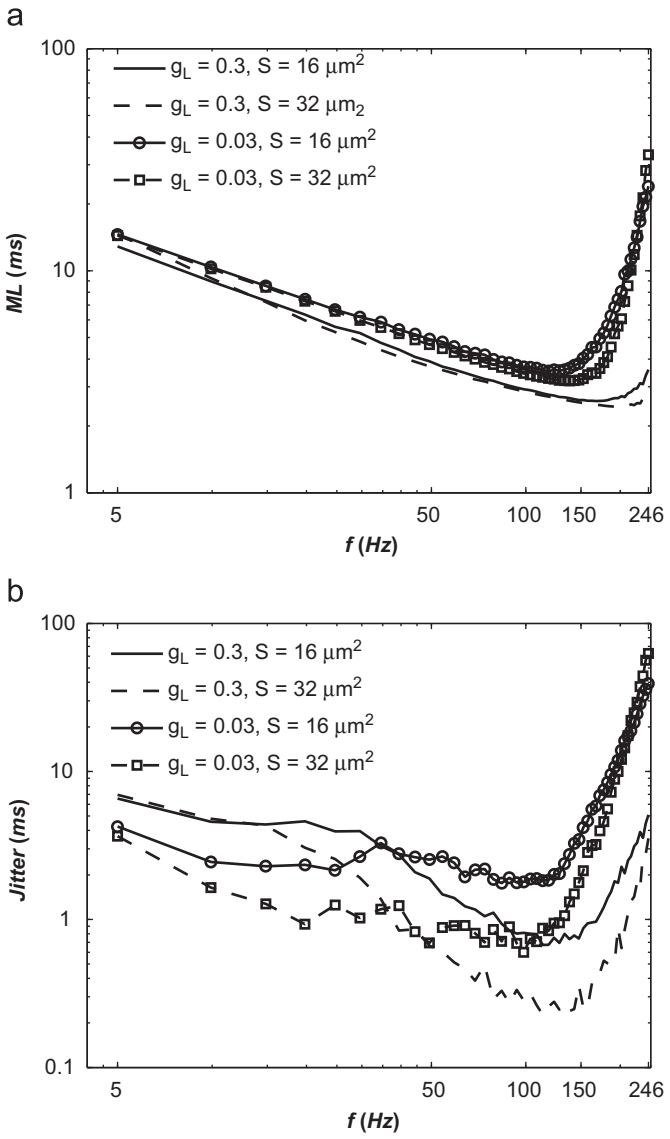

Fig. 7. The statistics of the latency for two different patch sizes (16 and 32 μm^2) and two different leakage conductance 0.3 mS cm^{-2} and 0.03 mS cm^{-2}, corresponding to the time constants of 3.3 and 33 ms, respectively: (a) the mean latency versus the frequency and (b) the temporal jitter versus the frequency.

For the suprathreshold input of 160 Hz, first spike jitter as a function of initial phase exhibits very different characteristics as compared to the mean latency. In particular, when the patch size is very small, jitter is almost independent of the initial phase, but as the patch size increases jitter becomes strongly dependent on initial phase. Similarly to the mean latency, for small noise the jitter first decreases with the initial phase, reaches a minimum for initial phases around $\pi/5$ and $\pi/3$, (with larger optimal phases for lower noise values) and then increases for initial phases up to $\phi = \pi/2$. For the larger patch sizes the optimal initial phases give roughly a 1.4-fold decrease in the jitter compared to $\phi = 0$. Furthermore, for the larger patches the jitter displays a pronounced peak at about $\phi = 3\pi/5$, giving a 30-fold increase in the jitter compared to $\phi = 0$ [Fig. 5(b)]. A further increase in the initial phase decreases the jitter and results in another minimum at around $\phi = \pi$ for the larger patch sizes.

In this context, Pankratova et al. (2005b) obtained the mean latency as a function of input frequency for the suprathreshold regime, averaged over all values of the initial phase (their Fig. 7), reporting an increase of the mean latency for all frequencies of the suprathreshold region as compared to the case when the initial phase of the input was zero. Our result in Fig. 5 explains this result graphically by showing that the mean latencies as a function of input phase for all patch sizes, as compared to $\phi = 0$, take larger values for a range around $\phi = 0.7\pi$–2π, with only slightly smaller latencies seen for a small range of initial phases around $\phi = 0$–$\pi/2$. As a result, for all values of the channel noise, the phase-averaged mean latency leads to an increase of the mean latency.

3.4. Dependence of latency and jitter on the membrane time constant

The effective membrane time constant of a neuron depends on the activity of its synaptic input, thus the network state (Rudolph and Destexhe, 2006). To see how network activity can modulate latency and jitter, we investigated the effect of the membrane time constant on these parameters for two patch sizes, 16 and 32 μm^2, with a value for the leakage conductance used in the previous simulations, 0.3 mS cm^{-2}, and a value ten times smaller, 0.03 mS cm^{-2}, corresponding to the time constants of 3.3 and 33 ms, respectively (Fig. 7).

The larger time constant of 33 ms shifts the boundaries of the sub and suprathreshold frequency regions towards lower values, such that the suprathreshold frequency range covers a range of 0.1–246 Hz, compared to the range of 5–350 Hz for a time constant of 3.3 ms. We then compared the dependency of the latency on the membrane time constant for the suprathreshold region common to both values of the time constant, thus 5–246 Hz, as can be inferred from Fig. 7(a). For both patch sizes, the minima of the mean latencies for the time constant of 33.3 ms (120 Hz, patch size of 16 μm^2; 150 Hz, patch size of 32 μm^2) are at lower frequencies as compared to those for 3.3 ms. From this result we can conclude that a reduction in membrane time constant provides a broader parameter range for processing high-frequency stimuli up to 200 Hz, above which the input is essentially ignored. The mean latency is slightly larger with the larger time constant for frequencies up to the minimum latency frequency, and then much larger for frequencies above this value. For example, at a frequency of 246 Hz, for a patch size of 16 μm^2 mean latencies were 3.5 and 24 ms for membrane time constants of 3.3 and 33 ms, respectively, and for a patch size 32 μm^2 were 3 and 33 ms for time constants of 3.3 and 33 ms, respectively.

In comparison to the effects on spike latency, the impact of the membrane time constant on first spike jitter is more diverse [Fig. 7(b)]. For both patch sizes, jitter is larger for a membrane time constant of 3.3 ms compared to a time constant of 33 ms for inputs up to about 40 Hz. Above 40 Hz, the relation reverses, with the jitter being larger for the larger membrane time constant. In this frequency range the jitter shows an overall dependence on input frequency resembling that for the mean latency, showing a minimum value that depends on noise strength, being larger for stronger channel noise, as shown earlier. The minimum jitter for the faster time constant is more sharply tuned than for the larger time constant, in the latter case being relatively constant over a band of frequencies between 20 and 130 Hz. These results suggest that the resonance characteristic of the minimum jitter, which is in agreement with previous studies related to cortical cells (Fellous et al., 2001; Gutkin et al., 2003), are significantly degraded as the membrane time constant increases.

4. Discussion

Studying the response of a neuron to periodic stimulation offers an important approach for examining its intrinsic dynamics, and for investigating information encoding and transmission of the nervous system at the cellular level (Kaplan et al., 1996; Hooper, 1998; Segundo et al., 1998; Szücs et al., 2001; Fellous et al., 2001; Schmid et al., 2003; Ozer, 2006; Ozer et al., 2006, 2008; Brumberg and Gutkin, 2007). In the current work we investigated how the frequency and the initial phase of the periodic forcing determine response latency and jitter of isolated neuronal membrane patches which include intrinsic noise from stochastic Hodgkin–Huxley type ion channels. Our results suggest non-trivial firing behavior for these membranes, which may correspond to so-called "hot spots" (Meunier and Segev, 2001; Kosaka et al., 2008) or otherwise spatially restricted regions (e.g. thin axons, Faisal and Laughlin, 2007, or dendritic spines, Segev and Rall, 1998) in dendritic or axonal trees, where either strongly inhomogeneous distributions of channels or significant electrotonic isolation validate the approximation of isolated patches as studied here.

In the absence of noise and for a sinusoidal input, the threshold current for firing of a Hodgkin–Huxley model depends on frequency (Schmid et al., 2003). Thus, as the frequency increases from zero, a sinusoidal input of a given (minimum) amplitude is subthreshold, then suprathreshold, and the subthreshold again. By considering a biophysically realistic model, we were able to relate the membrane area (and thus the level of intrinsic noise) to the latency in a manner that more closely mimics actual conditions with conductance noise, as compared to a model with additive current noise as used by Pankratova et al. (2005b).

Our results indicate that channel noise decreases the mean latency and jitter of the first spikes in response to subthreshold forcing—corresponding to the first and third input frequency regions—where the neuronal membrane only fires in the presence of noise. The sensitivity of response timing to noise strength is greater for subthreshold than suprathreshold frequency inputs, which follows from the fact that noise is necessary for spiking for subthreshold inputs. In general, we find that spike latency is dependent on both frequency and channel noise within the first subthreshold region, with the frequency dependence dominating over the noise dependence as the frequency increases. As the input enters the intermediate suprathreshold frequency region, spike latency and jitter is relatively insensitive to frequency in the presence of large channel noise, but still sensitive to frequency when the noise is small. For inputs in the third subthreshold frequency region, mean latency is sensitive mainly to channel noise and only very weakly sensitive to the frequency, corresponding to the fact that as the frequency increases the input has a vanishing influence on firing.

In the two subthreshold regions jitter takes relatively large values, compared to the suprathreshold region, with values comparable to the mean latency for a given channel noise strength. Response timing sensitivity to noise strength overall is greater for subthreshold frequency inputs, which is not surprising since noise provides a necessary drive for spiking for these frequencies. Since the input has little effect on response for the third subthreshold region, taken together these results support the idea that noisy spike encoders in realistic environments prefer inputs that vary slowly in time (Steinmetz et al., 2001), but with the constraint that the forcing is subthreshold. Thus, in terms of the latency the subthreshold dynamics seems to be similar to that of a low-pass filter.

Within the intermediate suprathreshold frequency range, the frequency dependence of both mean latency and jitter exhibits a resonance-like behavior, with channel noise increasing latency and jitter over a substantial portion of this region. For inputs near the resonance frequency that gives the minimum latency and jitter, increasing channel noise increases jitter, whereas for input frequencies far from the resonance, noise has the opposite effect on precision, such that increasing channel noise decreases jitter. Thus, there is an optimal range of stimulus frequencies that evoke a precisely timed first spike, depending on the level of noise, similar to the behavior of the stochastic θ-neuron model, a reduced model of cortical neurons (Gutkin et al., 2003).

We also examined effects of the initial phase of the periodic forcing on spike latency. Although the driving of a neuron by a stimulus that is suddenly switched on at time zero, corresponding to a non-zero initial phase, may seem unrealistic, step responses (e.g. to current) are classical protocols in electrophysiology and, more importantly, abrupt changes in the input are quite common in realistic situations (Geritner and Kistler, 2002). We found diverse effects of initial phase on the first spike time encoding, with the dependence of latency depending on both input frequency and the noise strength. An important finding of the present work is that the initial phase of the input provides an additional resonant behavior with respect to a minimum of the mean latency, occurring at initial phases that range up to $\phi = \pi/2$, depending on the frequency of the input and the amplitude of the channel noise. We also found a range of initial phases for the first region of subthreshold input frequencies where channel noise increases the mean latency and jitter, while for another range of

initial phases in the second suprathreshold region of input frequencies the channel noise decreases only the mean latency and not the jitter. For input in the third, high frequency subthreshold range, the response timing was relatively insensitive to initial input phase.

Given that a neuron fires periodically and thus behaves as a neural oscillator, it can be described by a phase of its firing. In this case, the phase-response curve (PRC) is used to determine how a perturbative (brief and weak) input, injected at a given phase within the interspike interval, advances or delays the successive spike generation of the oscillator (Gutkin et al., 2005; Brumberg and Gutkin, 2007; Tsubo et al., 2007). Therefore, the PRC reflects how the relative phase of the input affects such a phase-shift in the response of a periodically firing neuron. In the present case, although it may be implicitly related, we addressed a different subject and focused on the impact of the initial phase of periodic stimulus on spike latency and jitter in response to the subthreshold and suprathreshold inputs. We also changed the cells size, and thereby the strength of internal noise level for each case, leading to variations in the firing rate in the absence of external stimulus, and determined the impact of the initial phase of periodic stimulus on the first spike response of the single neuron with a variable size. Although it is beyond the scope of the present study, in order to relate the phase of latency or the phase of jitter to the phase of input in the context of the PRC, one must consider the only suprathreshold region with a given background suprathreshold dc current (or the level of excitability), and apply a weak and brief stimulus at a given phase within the first-spike time and then measure how the phase of this stimulus affect the phase of the first-spike latency.

Pankratova et al. (2005b) suggested that the choice of a certain frequency range makes it possible to minimize the delay in signal detection. However, we found a wide optimal frequency band for optimal first spike responses, compared to a more narrow band in the model of Pankratova et al. (2005b). It thus seems likely that the difference stems from the dynamic differences between neuronal models driven by current noise as in Pankratova et al. (2005b) versus conductance noise as used in the present study. This suggests that stochastic ion channels of neuronal membranes may enhance the range of input frequencies for effective detection of the first spikes. In addition, we also show that there is an optimal range of the initial phase that decreases the mean latency for a given channel noise strength. We suggest that specific ranges of input frequency and initial phase range allows a further minimization of the signal detection delay in a stochastic neuronal membrane. Pankratova et al. (2005b) also showed that noise increases the system's response time for all suprathreshold frequencies of the input. However, by using a more realistic model we showed that in the suprathreshold region the channel noise has a detrimental effect only within 18–300 Hz, whereas it has a constructive effect by decreasing both the mean latency and jitter outside this frequency range.

Finally, we investigated the dependence of the first spike timing and jitter on the membrane time constant and found that a higher time constant destroys the strong resonance behavior of the jitter by providing a plateau region whose magnitude increases with increasing strengths of the channel noise. We also find that lower time constants result in a broader parameter range for resolving high frequency stimuli.

Acknowledgments

This work was supported by a grant from The Scientific and Technological Research Council of Turkey (TUBITAK), 219.01-880-5768 to Mahmut Ozer, and a HFSP Grant (RGP0049/2002) and an Agence Nationale Recherche Grant (FUNVISYNIN) to Lyle J. Graham. Matjaž Perc acknowledges support from the Slovenian Research Agency (Grant Z1-9629). The authors would like to thank to Boris Gutkin for valuable discussions and detailed comments on the manuscript.

References

Bezrukov, S.M., Vodyanov, I., 1995. Noise-induced enhancement of single transduction across voltage-dependent ion channels. Nature 378, 362–364.
Brumberg, J.C., Gutkin, B.S., 2007. Cortical pyramidal cells as non-linear oscillators: experiment and spike-generation theory. Brain Res. 1171, 122–137.
Butts, D.A., Weng, C., Jin, J., Yeh, C.I., Lesica, N.A., Alonso, J.M., Stanley, G.B., 2007. Temporal precision in the neural code and the time scales of natural vision. Nature 449, 92–95.
Chen, W., Zhang, J.J., Hu, G.Y., Wu, C.P., 1996. Electrophysiological and morphological properties of pyramidal and nonpyramidal neurons in the cat motor cortex in vitro. Neuroscience 73, 39–55.
Chow, C.C., White, J.A., 1996. Spontaneous action potentials due to channel fluctuations. J. Biophys. 71, 3013–3021.
de Ruyter van Steveninck, R., Bialek, W., 1988. Real-time performance of a movement sensitive neuron in the blowfly visual system: coding and information transfer in short spike sequences. Proc. R. Soc. London Ser. B 234, 379–414.
Faisal, A.A., Laughlin, S.B., 2007. Stochastic simulations on the reliability of action potential propagation in thin axons. PLoS Comput. Biol. 3, e79.
Fellous, J.M., Houweling, A.R., Modi, R.H., Rao, R.P.N., Tiesinga, P.H.E., Sejnowski, T.J., 2001. Frequency dependence of spike timing reliability in cortical pyramidal cells and interneurons. J. Neurophysiol. 85, 1782–1787.
Fox, R.F., 1997. Stochastic versions of the Hodgkin–Huxley equations. J. Biophys. 72, 2068–2074.
Geritner, W., Kistler, W.M., 2002. Spiking Neuron Models: Single Neurons Populations Plasticity. Cambridge University Press, Cambridge.
Gutkin, B., Ermentrout, G.B., Rudolph, M., 2003. Spike generating dynamics and the conditions for spike-time precision in cortical neurons. J. Comput. Neurosci. 15, 91–103.
Gutkin, B.S., Ermentrout, G.B., Reyes, A.D., 2005. Phase-response curves give the responses of neurons to transient inputs. J. Neurophysiol. 94, 1623–1635.
Heil, P., 2004. First-spike latency of auditory neurons revisited. Curr. Opin. Neurobiol. 14, 461–467.
Hodgkin, A.L., Huxley, A.F., 1952. A quantitative description of membrane current and its application to conduction and excitation in nerve. J. Physiol. (London) 117, 500–544.
Hooper, S.L., 1998. Transduction of temporal patterns by single neurons. Nat. Neurosci. 1, 720–726.
Hunter, J.D., Milton, J.G., Thomas, P.J., Cowan, J.D., 1998. Resonance effect for neuronal spike time reliability. J. Neurophysiol. 80, 1427–1438.
Jung, P., Shuai, J.W., 2001. Optimal size of ion channel clusters. Europhys. Lett. 56, 29–35.
Kaplan, D.T., Clay, J.R., Manning, T., Glass, L., Guevara, M.R., Shrier, A., 1996. Subthreshold dynamics in periodically stimulated squid axons. Phys. Rev. Lett. 76, 4074–4077.
Kosaka, T., Komada, M., Kosaka, K., 2008. Sodium channel cluster, [beta] IV-spectrin and ankyrinG positive 'hot spots' on dendritic segments of parvalbumin-containing neurons and some other neurons in the mouse and rat main olfactory bulbs. Neurosci. Res. 62, 176–186.
Kruger, J., Becker, J.D., 1991. Recognizing the visual stimulus from neuronal discharges. Trends Neurosci. 14, 282–285.
Lecar, H., Nossal, R., 1971. Theory of threshold fluctuations in nerves. I: relationships between electrical noise and fluctuations in axon firing. J. Biophys. 11, 1048–1067.
Levin, J.E., Miller, J.P., 1996. Broadband neural encoding in the cricket cercal sensory system enhanced by stochastic resonance. Nature 380, 165–168.
Meunier, C., Segev, I., 2001. Neurones as physical objects: structure, dynamics and function. In: Moss, F., Gielen, S. (Eds.), Handbook of Biological Physics, vol. 4. Elsevier, London, pp. 353–466.
Middlebrooks, J.C., Clock, A.E., Xu, L., Green, D.M., 1994. A panoramic code for sound location by cortical neurons. Science 264, 842–844.
Mino, H., Rubinstein, J.T., White, J.A., 2002. Comparison of algorithms for the simulation of action potentials with stochastic sodium channels. Ann. Biomed. Eng. 30, 578–587.
Ozer, M., Ekmekci, N.H., 2005. Effect of channel noise on the time-course of recovery from inactivation of sodium channels. Phys. Lett. A 338, 150–154.
Ozer, M., 2006. Frequency-dependent information coding in neurons with stochastic ion channels for subthreshold periodic forcing. Phys. Lett. A 354, 258–263.
Ozer, M., Uzuntarla, M., Agaoglu, S.N., 2006. Effect of the subthreshold periodic current forcing on the regularity and the synchronization of neuronal spiking activity. Phys. Lett. A 360, 135–140.
Ozer, M., Graham, L.J., 2008. Impact of network activity on noise delayed spiking for a Hodgkin–Huxley model. Eur. Phys. J. B 61, 499–503.
Ozer, M., Uzuntarla, M., Kayikcioglu, T., Graham, L.J., 2008. Collective temporal coherence for subthreshold signal encoding on a stochastic small-world Hodgkin–Huxley neuronal network. Phys. Lett. A 372, 6498–6503.

Ozer, M., Perc, M., Uzuntarla, M., 2009. Stochastic resonance on Newman–Watts networks of Hodgkin–Huxley neurons with local periodic driving. Phys. Lett. A 373, 964–968.
Pankratova, E.V., Polovinkin, A.V., Spagnolo, B., 2005a. Suppression of noise in FitzHugh–Nagumo model driven by a strong periodic signal. Phys. Lett. A 344, 43–50.
Pankratova, E.V., Polovinkin, A.V., Mosekilde, E., 2005b. Resonant activation in a stochastic Hodgkin–Huxley model: interplay between noise and suprathreshold driving effects. Eur. Phys. J. B 45, 391–397.
Panzeri, S., Petersen, R.S., Schultz, S.R., Lebedev, M., Diamond, M.E., 2001. The role spike timing in the coding of stimulus location in rat somatosensory cortex. Neuron 29, 769–777.
Philips, D.P., 1998. Factors shaping the response latencies of neurons in the cat's auditory cortex. Behav. Brain Res. 93, 33–41.
Rowat, P.F., Elson, R.C., 2004. State-dependent effects of Na channel noise on neuronal burst generation. J. Comput. Neurosci. 16, 87–112.
Rubinstein, J.T., 1995. Threshold fluctuations in an *N* sodium channel model of the node of Ranvier. J. Biophys. 68, 779–785.
Rudolph, M., Destexhe, A., 2006. Event-based simulation strategy for conductance-based synaptic interactions and plasticity. Neurocomputing 69, 1130–1133.
Schmid, G., Goychuk, I., Hanggi, P., 2001. Stochastic resonance as a collective property of ion channel assemblies. Europhys. Lett. 56, 22–28.
Schmid, G., Goychuk, I., Hanggi, P., 2003. Membrane clusters of ion channels: size effects for stochastic resonance. In: Pastor-Satorras, R., Rubi, M., Diaz-Guilera, A. (Eds.), LNP, vol. 625, pp. 195–206.
Schmid, G., Goychuk, I., Hanggi, P., Zeng, S., Jung, P., 2004. Stochastic resonance and optimal clustering for assemblies of ion channels. Fluct. Noise. Lett. 4, 33–42.
Schmid, G., Hanggi, P., 2007. Intrinsic coherence resonance in excitable membrane patches. Math. Biosci. 207, 235–245.
Schneidman, E., Freedman, B., Segev, I., 1998. Ion channel stochasticity may be critical in determining the reliability and precision of spike timing. Neural Comput. 10, 1679–1703.
Schneidman, E., Segev, I., Tishby, N., 2000. Information capacity and robustness of stochastic neuron models. In: Sollo, S.A., et al. (Eds.), Advances in Neural Information Processing Systems, pp. 178–184.
Segev, I., Rall, W., 1998. Excitable dendrites and spines: earlier theoretical insights elucidate recent direct observations. Trends Neurosci. 21, 453–460.
Segundo, J.P., Sugihara, G., Dixon, P., Stiber, M., Bersier, L.F., 1998. The spike trains of inhibited pacemaker neurons seen through the magnifying glass of nonlinear analyses. Neuroscience 87, 741–766.
Sigworth, F.J., 1980. The variance of sodium current fluctuations at the node of Ranvier. J. Physiol. (London) 307, 97–129.
Skaugen, E., Walloe, L., 1979. Firing behaviour in a stochastic nerve membrane model based upon the Hodgkin–Huxley equations. Acta Physiol. Scand. 107, 343–363.
Steinmetz, P.N., Manwani, A., Koch, C., 2001. Variability and coding efficiency of noisy neural spike encoders. Biosystems 62, 87–97.
Strassberg, A.F., DeFelice, L.J., 1993. Limitations of the Hodgkin–Huxley formalism: effects of single channel kinetics on trans-membrane voltage dynamics. Neural Comput. 5, 843–855.
Szücs, A., Elson, R.C., Rabinovich, M.I., Abarbanel, H.D.I., Selverston, A.I., 2001. Nonlinear behavior of sinusoidally forced pyloric pacemaker neurons. J. Neurophysiol. 85, 1623–1638.
Tovée, M.J., Rolls, E.T., Treves, A., Bellis, R.P., 1993. Information encoding and the response of single neurons in the primate temporal visual cortex. J. Neurophysiol. 70, 640–654.
Tsubo, Y., Takada, M., Reyes, A.D., Fukai, T., 2007. Layer and frequency dependencies of phase response properties of pyramidal neurons in rat motor cortex. Eur. J. Neurosci. 25, 3429–3441.
Tuckwell, H.C., 2005. Spike trains in a stochastic Hodgkin–Huxley system. BioSytems 80, 25–36.
Tuckwell, H.C., Wan, F.Y.M., 2005. Time to first spike in stochastic Hodgkin–Huxley systems. Physica A 351, 427–438.
Vanrullen, R., Guyonneau, R., Thorpe, S.J., 2005. Spike times make sense. Trends Neurosci. 28, 1–4.
White, J.A., Rubinstein, J.T., Kay, A.R., 2000. Channel noise in neurons. Trends Neurosci. 23, 131–137.
Yang, L., Jia, Y., 2005. Effects of patch temperature on spontaneous action potential train due to channel fluctuations: coherence resonance. Biosystems 81, 267–280.